

Impact of initial conditions on hysteretic behaviour of the boost converter

D.Pelin, M.Ručević, D.Vulin

Josip Juraj Strossmayer University of Osijek, Faculty of Electrical Engineering , Osijek, Croatia, dpelin@etfos.hr

Abstract— The different steady-state responses of a boost converter are observed during measurements carried out on the physical model of the chosen boost converter. It is shown that by varying the input voltage only, the boost converter exhibits hysteretic behavior. The various set of steady-state responses are recognized by increasing the dc input voltage regarding the set of steady state responses which are obtained by decreasing the dc input. Also, the steady-state responses of the boost converter are determined by means of computer simulation and presented in figure of bifurcation diagram. The results of computer simulation and results of experiment coincide very well for one trend of varying input voltage only. Therefore, impact of initial conditions of the state variables in the form of bifurcation diagram is studied.

Keywords — boost converter, steady-state responses, hysteretic behaviour, impact of initial condition.

I. INTRODUCTION

The boost converters are time-varying nonlinear dynamical systems [1-3] exhibiting several steady-state responses, from subharmonic responses as well as quasiperiodic responses to chaos [4-6]. The transitions between steady-state responses are strongly dependent on the converter parameter choice [7-10]. In the research of steady-state responses of the DC-DC converters the experimental studies are often used approach [11-13].

The correct design of the boost converters assumes that all possible steady-state responses and their dependence on variation of converter parameters are known in advance. In this way it is possible to avoid occurrence of some undesirable properties during service like increased output ripple or audible sound.

In the paper computer simulation and experiments carried out on the physical model of the converter have been used and presented. Simulation results are presented by waveforms of state variables and by bifurcation diagram. Measurements are presented as waveforms of steady state variables and control voltage. It is shown that different set of steady-states were obtained by increasing the dc input voltage relating to the set of steady states which were obtained by decreasing the dc input voltage throughout experiment. This characteristic behavior of the boost converter which is dependent on trend of the varying input voltage we called hysteretic behavior.

The steady-state analysis obtained by using the mathematical model of the boost converter is verified for one set of steady-state responses, which agree to the decreasing input voltage only.

In our study of steady-state behaviour of the boost converter a special attention is paid to the explanation of

discrepancy between measurement results and simulation results. Therefore, the impact of initial conditions on hysteretic behaviour of the boost converter is studied by using bifurcation diagrams with initial values of state variables as bifurcation parameters. In our opinion, the initial conditions are parameters of converter which can't be controlled during measurements.

II. BOOST CONVERTER REALIZATION

The boost converter controlled by naturally-sampled constant frequency pulse-width, low-cost modulator MC34060A is realized, Fig.1. The realization of the given boost converter was taken over from the datasheet-catalog of MC34060A [14]. The typical values for the boost converter realization are: input voltage; 7V- 40V, maximum output voltage; 40V, typical frequencies; 1kHz-200kHz; typical power; $\leq 100W$. The average value of output voltage was set from 26.5V to 27.5V and was depended of the characteristic steady-state responses.

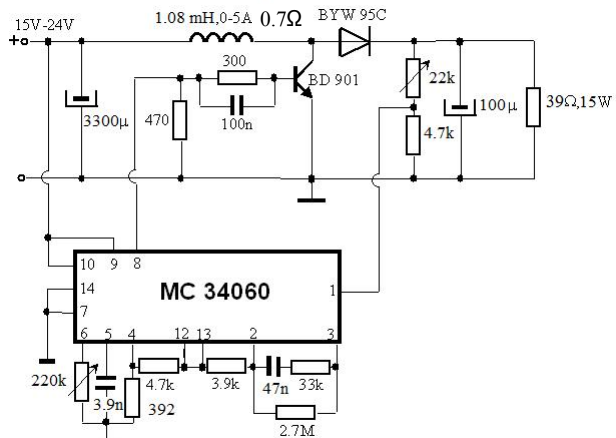


Fig. 1. Schematic of the experimental boost converter.

The controlled switch is realized by the bipolar transistor BDY 901 and the uncontrolled switch by the diode BYW 95C. The low switching frequency, $f=5\text{ kHz}$, guarantees that high-frequency effects are minimized. The choke is designed with characteristic inductance L ; $L=1.08\text{mH}$ and characteristic resistance, R ; $R=0.7\Omega$. In this way the converter is made closer to ideal and therefore easier to compare results of measurements with simulation results.

III. HYSTERETIC BEHAVIOUR

The characteristic steady-state responses were identified by comparing the waveforms of inductor current; i_L and output voltage u_C simultaneously with

sawtooth ramp voltage, u_{ramp} , as one of the control voltage for operating pulse-width modulator, MC34060A.

TABLE I
REGIONS OF STEADY-STATE RESPONSES OF THE BOOST CONVERTER BY VARYING INPUT VOLTAGE

Increasing $E; \downarrow$		Decreasing $E; \uparrow$	
$E(V)$	Steady-state	$E(V)$	Steady-state
17-22.5	Period-one operation, \downarrow		
22.5-23.1	Period-two operation, \downarrow	17.-23.02	Period-three operation,
23.1-23.45	Period-six operation, \downarrow	23.02-23.38	Period-six operation, \uparrow
23.45-24.28	Chaos, \downarrow	23.38-24.02	Chaos, \uparrow
23.28-24.55	Period-four operation, \downarrow	24.02-24.39	Period-four operation, \uparrow
24.55-24.64	Period-eight operation, \downarrow	24.39-24.59	Period-eight operation, \uparrow
24.64-25.57	Chaos, \downarrow	24.59-25.53	Chaos, \uparrow
25.57-25.86	Period-five operation, \downarrow	25.53-25.83	Period-five operation, \uparrow
25.86-26.80	Chaos, \downarrow	25.83-26.62	Chaos, \uparrow
26.80-26.98	Period-six operation, \downarrow	26.62-27	Period-six operation, \uparrow
26.98-27	Chaos		

The steady-state responses of the boost converter are identified by increasing the input voltage, E from 17V to 27V and also by decreasing the input voltage, E from 27V to 17V. The results obtained by measurements are shown in Table 1. The tendency off appearing the steady-states is denoted with symbol “ \downarrow ”, for increasing input voltage and with symbol “ \uparrow ”, for decreasing input voltage.

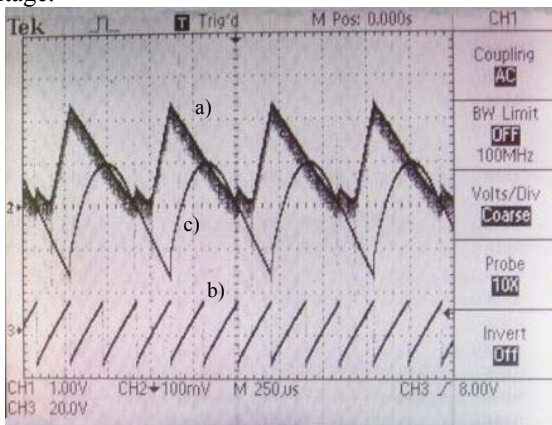


Fig. 2. Period-three; ($E=22.77V$, $U_c(0)=27.16V$), increasing $E; \downarrow$

- a) Measured inductor current, i_L ; (1A/div)
- b) Measured sawtooth ramp voltage, u_{ramp} (2V/div),
- c) Measured AC component of output voltage, u_c (1V/div)

The hysteretic behavior [15] of the boost converter can be easily recognized from Table 1. The set of the steady-states which have appeared in the same order irrespectively to the trend of varying input voltage is denoted with grey shading in the Table 1. The hysteresis of the steady-state responses was noticed at the critical values of the input voltage from 23.02 V to 23.15 V.

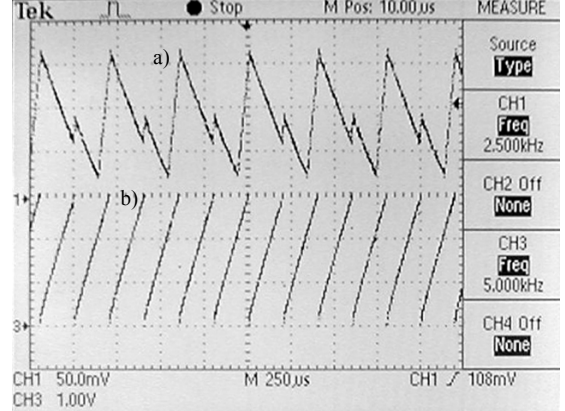


Fig. 3. Period -two($E=22.77V$, $U_c(0)=26.95V$), decreasing $E; \uparrow$
a) Measured inductor current, i_L ; (1A/div),
b) Measured sawtooth ramp voltage, u_{ramp} (1V/div).

The waveforms of inductor current, i_L and sawtooth ramp voltage, u_{ramp} for the same value of input voltage ($E=22.77V$), but for the different trend of changing input voltage are shown on Fig.2.-3. Two different steady-state responses are identified: period-three operation for decreasing input voltage and period-two operation for increasing input voltage.

IV. STATE EQUATIONS

The equivalent circuit of the realized boost converter is shown in Fig.4. The discontinuous conduction mode as well as continuous conduction mode are assumed, i.e. there are three/two changes of power circuit topology in a period of operation $T=1/f$.

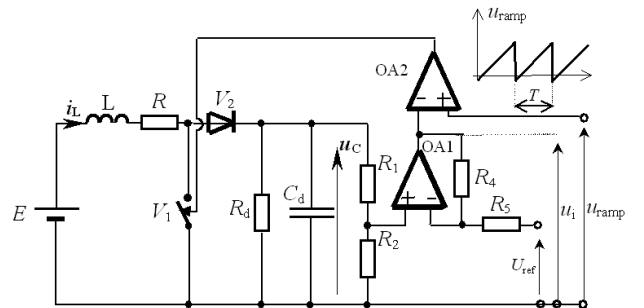


Fig. 4. The equivalent circuit of the boost converter

Therefore, the boost converter can be modeled by piece-wise linear time-varying network which passes in a period of operation T through three/two different configuration.

When $u_{ramp} \geq u_i$, the controlled switch V_1 is in the ON-state and the diode V_2 is in the OFF-state. The state equations are:

$$\begin{aligned}\frac{du_C}{dt} &= \frac{1}{CR_d} u_C \\ \frac{di_L}{dt} &= \frac{1}{L}(E - Ri_L)\end{aligned}\quad (1)$$

When $u_{\text{ramp}} < u_i$, $i_L > 0$, the controlled switch V_1 is in the OFF-state and the diode V_2 is in the ON-state. The state equations are:

$$\begin{aligned}\frac{du_C}{dt} &= \frac{1}{C} \left(i_L - \frac{u_C}{R_d} \right) \\ \frac{di_L}{dt} &= \frac{1}{L} (E - R_i_L - u_C)\end{aligned}\quad (2)$$

When $u_{\text{ramp}} < u_i$, $i_L = 0$, the controlled switch V_1 and the diode V_2 are in the OFF-state. The state equations are:

$$\begin{aligned}\frac{du_C}{dt} &= \frac{1}{CR_d} u_C \\ i_L &= 0\end{aligned}\quad (3)$$

According to Fig.4 the input voltage of the operational amplifier OA2 $u_i(t)$ is given by

$$u_i = \frac{-R_4}{R_5} U_{\text{ref}} + \left(1 + \frac{R_4}{R_5} \right) \cdot \frac{R_2}{R_1 + R_2} u_C \quad (4)$$

The external sawtooth ramp voltage:

$$u_{\text{ramp}} = \frac{3}{T} t + 0.7 \text{ [V]} \quad (5)$$

is obtained by measurements carried out on the pulse-width modulator MC34060A.

V. COMPARING SIMULATION RESULTS WITH MEASUREMENTS

All simulations are carried out for a fixed set of converter parameters: $R_1=22\text{k}\Omega$, $R_2=1.22\text{k}\Omega$, $R_4=2.7\text{M}\Omega$, $R_5=3.9\text{k}\Omega$, $R=0.7\Omega$, $L=1.08\text{mH}$, $C=100\mu\text{F}$, $R_d=39\Omega$, $U_{\text{ref}}=5\text{V}$ and $T=200\text{\mu s}$. Three parameters are considered as bifurcation parameter: the input voltage E , the initial value of output voltage $u_C(0)$ and the initial value of inductor current $i_L(0)$. State equations are integrated by using the fourth-order Runge-Kutta numerical integration method. The program was written in "C++" programming language for solving state equations (1-3) and the results of computation were presented by using MATLAB. Simulation results were presented as waveforms of the state variables u_C and i_L and as bifurcation diagrams.

All steady-state variables are presented in time period from $140T$ to $150T$ with the initial conditions of state variables: $u_C(0)=27.20\text{V}$ and $i_L(0)=0\text{A}$.

For bifurcation diagram, presented on Fig.6, 250 samples of output voltage $u_C(t_k)$ for each value of the bifurcation parameter, taken at the instants $t_k=kT$; $k=101, 102, \dots, 350$ are displayed. Although the boost converter is at steady state after a few periods, the safety margin of 100 periods is accepted. In this way we are sure that period-N operation of the converter will be

represented by exactly N points on a bifurcation diagram. Also, 250 points dispersed between the maximum and the minimum value of sampled variable u_C indicates the chaos. It is irrelevant which state variables will be sampled for identification of steady-state responses. Bifurcation diagrams for the both state variables lead to the same dynamical behavior of the converter.

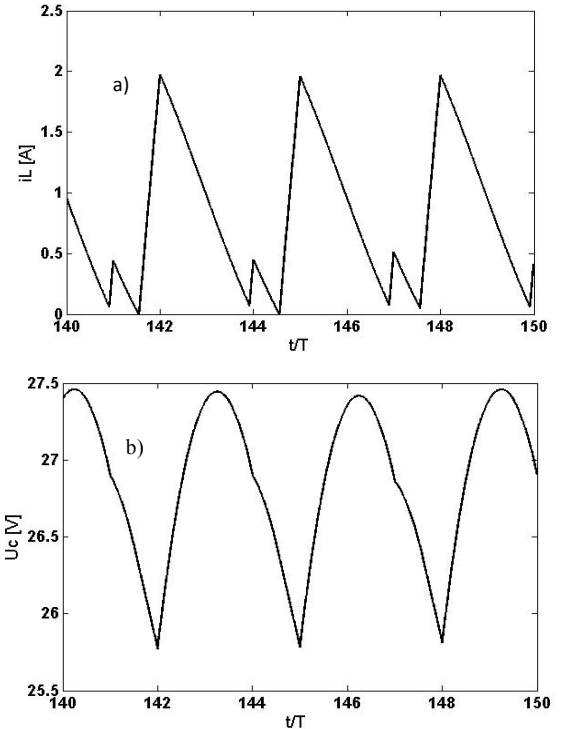


Fig. 5. Period- three operation
a) Computed inductor current, i_L at $E=22.77\text{ V}$,
b) Computed output voltage, u_C at $E=22.77\text{ V}$.

These computed results agree very well to the results obtained by measurements for decreasing input voltage only. The computed waveform of inductance current and output voltage which are shown on Fig.5., coincide very well to the measured waveforms which are shown on Fig.2. It looks like the mathematical model can be verified only for decreasing input voltage.

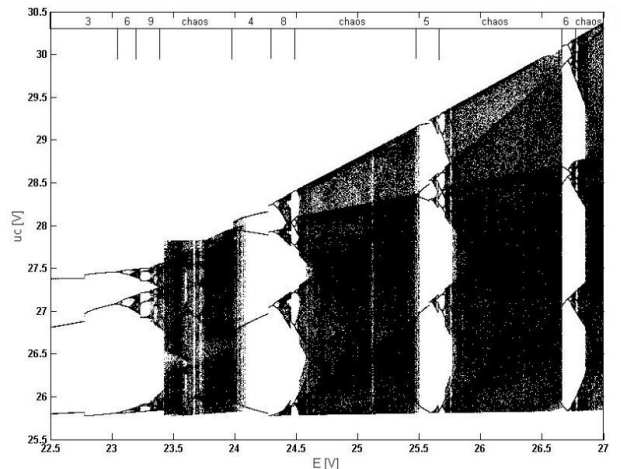


Fig. 6. Bifurcation diagram with the input voltage E as the bifurcation parameter. $E=22.5-27\text{V}$, $\Delta E=0.001\text{V}$

VI. IMPACT OF INITIAL CONDITIONS

It is supposed that the reason for different set of steady-state responses should be related to the impact of initial conditions. The initial conditions are parameters which can't be controlled in laboratory conditions. Therefore, ripple of the measured output voltage and the range of inductor current, Fig.2. were used as input values for computing bifurcation diagrams. For example, the average value of output voltage, $U_C(0)$ was 27.16 V. Then the maximum value of input voltage can be scan from Fig.2. and is equal to 28.16V and minimum value of output voltage is nearly about 25.51V. The minimal initial value of output voltage, $u_C(0)$ as bifurcation parameter is adjusted on 26.73V, Fig.8. The range of inductor current was acquired from 0 to 2.35A. These values were used as data for the initial values of inductor current, $i_L(0)$, as bifurcation parameter, Fig.7.

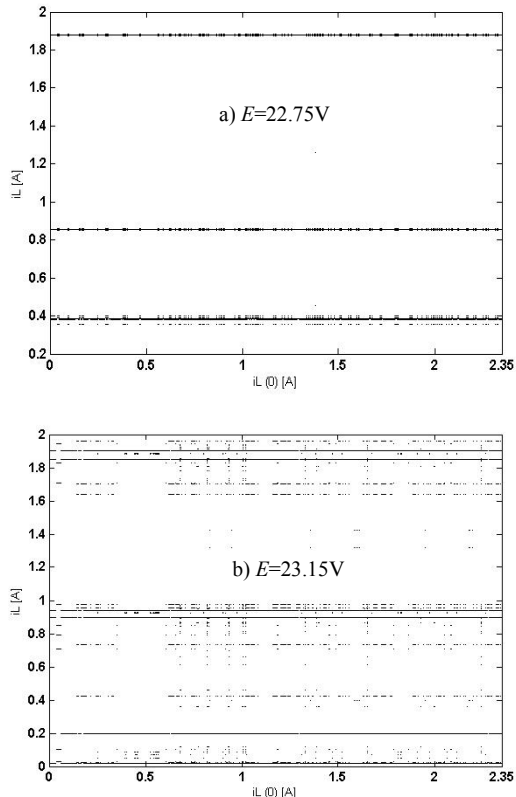


Fig. 7. Bifurcation diagrams with initial value of the inductor current $i_L(0)$ as bifurcation parameter; $i_L(0)=0\text{A}-2.35\text{A}$, $u_C(0)=26.95\text{V}$, $\Delta i_L(0)=0.001\text{A}$; a) $E=22.75\text{V}$, b) $E=23.15\text{V}$.

Bifurcation diagrams were computed in range of the critical value of input voltages, E of 22.75V to 23.15V with step size of input voltage of $\Delta E=0.1\text{V}$. Bifurcation diagrams for the inductor current, i_L as state variable for the two value of input voltage ($E=22.75\text{V}$ and critical value of input voltage $E=23.15\text{V}$) and for two bifurcation parameters (initial values of inductor current, $i_L(0)$ as well as initial value of output voltage, $u_C(0)$) are shown on Fig.7 and Fig.8.

The identification of steady-state responses from bifurcation diagrams was provided by using magnify details of the bifurcation diagrams, Fig.9.a and computed inductor currents as well as Poincaré maps Fig.9.b-9.c for the characteristic values of bifurcation parameter, $u_C(0)$.

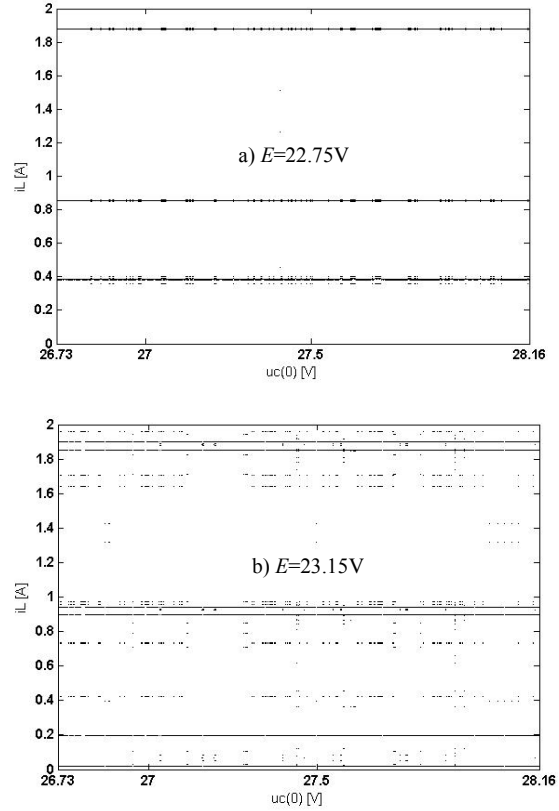


Fig. 8. Bifurcation diagram with initial value of the output capacitor voltage $u_C(0)$ as bifurcation parameter; $u_C(0)=26.7351\text{V}-28.16\text{V}$, $i_L(0)=0\text{A}$, $\Delta u_C(0)=0.001\text{V}$; a) $E=22.75\text{V}$, b) $E=23.15\text{V}$.

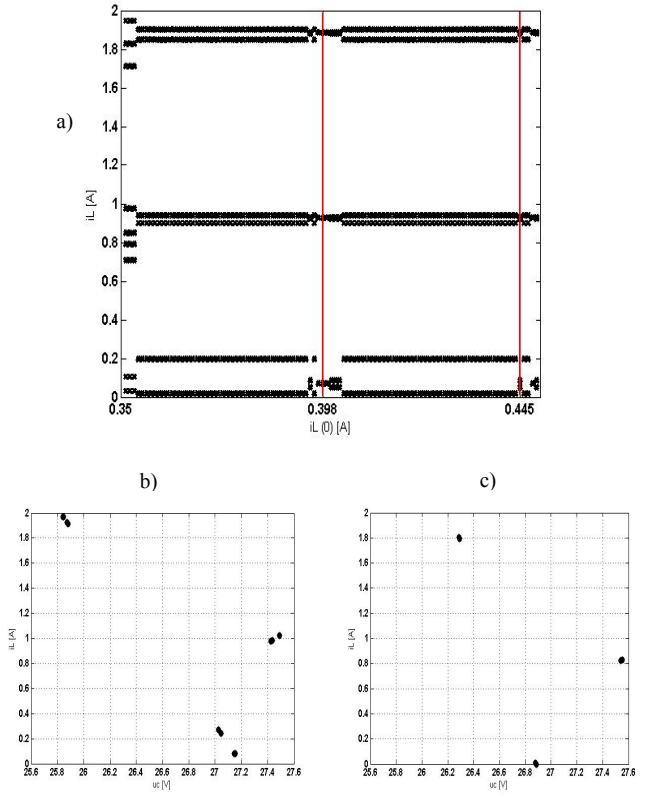


Fig. 9. a) The magnify detail of bifurcation diagram on the Fig 7b
b) Poincaré map at $i_L(0)=0.398\text{ A}$, period-six operation
c) Poincaré map at $i_L(0)=0.445\text{ A}$, period three operation.

The period-six operation was identified, Fig. 9.b. The period three-operation was also shown on Fig. 7.a and 8.a respectively. The period-two operation wasn't identified by analysis of the bifurcation diagrams for characteristic value of input voltage and step size of input voltage. It looks like the initial values of inductor current, $i_L(0)$ and initial values of output voltage, $u_C(0)$ are mutually more dependent. Also, existing of the different steady-state responses (period-two operation and period-three operation), for the same value of input voltage ($E=22.77V$) might be perhaps the physical characteristic of chosen boost converter[16].

VII. CONCLUSION

The hysteretic behavior was obtained for chosen boost converter by measurements. The proposed mathematical model of the boost converter can be used for prediction set of steady-state responses recognized by varying the input voltage in one tendency, only for decreasing input voltage.

The different steady-state responses; from period-three to period-six operation were identified by using analyzed bifurcation diagrams. The different steady-state responses are observed especially for the critical values of input voltage $E=23.02V \div 23.15V$ but the appearance of period-two operation, which was identified by measurements wasn't obtained by analysis of impact of initial conditions. Therefore, the mutual correlation between the initial conditions of inductor current, $i_L(0)$ as well as output voltage $u_C(0)$ with value of input voltage E would be more intensive.

Future work will include the analysis of impact of initial conditions at the appearance of steady-state responses on the critical values of input voltage. The parameter space maps with initial conditions and input voltage as bifurcation parameters will be researched.

REFERENCES

- [1] L.O.Chua, T.S.Parker: "Chaos: A tutorial for engineers", *Proceedings of the IEEE*, vol. 75, No. 8, pp. 982-1009, August 1987.
- [2] K.T.Alligood, T.D.Sauer, J.A York: "Chaos - introduction to dynamical systems", Springer-Verlag, New York 1996.
- [3] F.Moon: "Chaotic vibration", John Wiley and Sons, New York 1987.
- [4] C.K.Tse:"Bifurcation behaviour of DC/DC converters", CRC-Press, Hong-Kong, 2001
- [5] J.H.B.Deane, D.C.Hamill: "Instability, subharmonics and chaos in power electronic systems", *IEEE Transactions on Power Electronisc*, vol. 5, no. 3, pp. 260-268, July 1990.
- [6] M.Debbat,A.El Aroudi, R.Giral, L.Martinez-Salamero: "Hopf bifurcation in PWM controled asymetrical interleaved dual boost DC-DC converter," *Proceedings of IEEE International Conference of Industrial Technology*, pp. 860-865, Maribor, Slovenia, December 2004.
- [7] C.K.Tse, "Flip bifurcation and chaos in three-state boost switching regulators", *IEEE Transactions on Circuits and Systems-I*, vol.41, pp. 16-23, no.1, 1994.
- [8] K.W.E.Cheng, M.Liu, J.Wu: "Chaos study and parameter-space analysis of the DC-DC buck-boost converter," *IEE Proc.Electr.Power Application.*, vol. 150, no.2, pp. 126-138, March 2003.
- [9] E.Toribo, A.El Aroudi, G.Olivar, L.Benadero: "Numerical and experimental study of the region of period-one operation of a PWM boost converter", *IEEE Transactions on Power Electronic*, vol. 15, no. 6, pp. 1163-1171, November 2000.
- [10] I.Flegar, D.Pelin: "Steady-state responses of the boost converter," *Proceedings of IEEE International Conference of Circuits and Systems*, vol. 2, pp. 830-835, Dubrovnik, Croatia, July 2005.
- [11] D.Cafagna, G.Grassi: "Bifurcation Analysis and Chaotic Behaviour in Boost Converters: Experimental Results," *Nonlinear Dynamics*, vol. 44, pp. 251-262, 2006.
- [12] F.Angulo, C.Ocampo, G.Olivar, R.Ramos: "Nonlinear and nonsmooth dynamics in a DC-DC Buck converter:Two experimental set-ups," *Nonlinear Dynamics*, vol. 46, pp. 239-257, 2006.
- [13] K.W.E.Cheng, M.Liu, J.Wu: "Experimental study of bifurcation and chaos in the Buck-Boost converter," *IEE Proc.-Power Appl.* Vol.150. No.1., January, 2003.
- [14] Motorola Semiconductors: MC34060 datasheet, http://www.datasheetcatalog.com/datasheets_pdf/M/C/3/4/MC34060_0.shtml
- [15] D.Pelin, K.Miličević, A.Crnković: "Hysteretic behavior of the boost converter", *16th International Symposium on Power Electronics-Ee 2011*, Novi Sad, Serbia, October 2011, no.T1-1.4, pp. 1.-4.
- [16] S.Banerjee: "Coexisting attractors,chaotic saddles and fractal basins in power electronic circuit", *IEEE Transactions on Circuits and Systems-I*, vol. 44, no. 9, pp 847-849, Septembar1997.